Quantum conductance of graphene nanoribbons with edge defects

T. C. Li[1,2] and Shao-Ping Lu[1]
[1]*Department of Physics, The University of Texas at Austin, Austin, Texas 78712, USA*
[2]*Center for Nonlinear Dynamics, The University of Texas at Austin, Austin, Texas 78712, USA*
(Received 1 September 2006; published 6 February 2008)

The conductance of metallic graphene nanoribbons (GNRs) with single defects and weak disorder at their edges is investigated in a tight-binding model. We find that a single edge defect will induce quasilocalized states and consequently cause zero-conductance dips. The center energies and breadths of such dips are strongly dependent on the geometry of GNRs. Armchair GNRs are more sensitive to a vacancy than zigzag GNRs, but are less sensitive to a weak scatter. More importantly, we find that with a weak disorder, zigzag GNRs will change from metallic to semiconducting due to Anderson localization. However, a weak disorder only slightly affects the conductance of armchair GNRs.

DOI: 10.1103/PhysRevB.77.085408 PACS number(s): 73.63.−b, 72.10.−d, 81.05.Uw

I. INTRODUCTION

Recently, graphene (a single atomic layer of graphite) sheets were successfully isolated and demonstrated to be stable under ambient conditions.[1,2] Due to their unique two-dimensional (2D) honeycomb structures, their mobile electrons behave as massless Dirac fermions,[2–4] making graphene an important system for fundamental physics.[5–9] Moreover, graphene sheets have the potential to be lithographed to a lot of patterned graphene nanoribbons (GNRs)[10–15] to make large-scale integrated circuits.[16]

The electronic property of GNRs has attracted increasing attention. Recent studies[17–20] have shown that GNRs can be either metallic or semiconducting, depending on their shapes. This allows GNRs to be used as both connections and functional elements[21,22] in nanodevices, which is similar to carbon nanotubes (CNTs).[23,24]

However, GNRs are substantially different from CNTs by having two open edges at both sides (see Fig. 1). These edges not only remove the periodic boundary condition along the circumference of CNTs, but also make GNRs more vulnerable to defects than CNTs.[25,26] In fact, nearly all observed graphene edges[10,27,28] contain local defects or extended disorders, while few defects are found in the bulk of graphene sheets. These edge defects can significantly affect the electronic properties of GNRs. Edge states with energies about −0.1 to 0.2 eV have been observed.[27,28] Recent conductance measurements of GNRs also show that there are "inactive" ribbon widths in the charge transport due to localized edge states.[13] Theoretical studies of GNRs have also considered some edge corrections.[19,29–31] In this paper, we systematically study the conductance of metallic GNRs with single defects and weak disorder at edges using a tight-binding model.

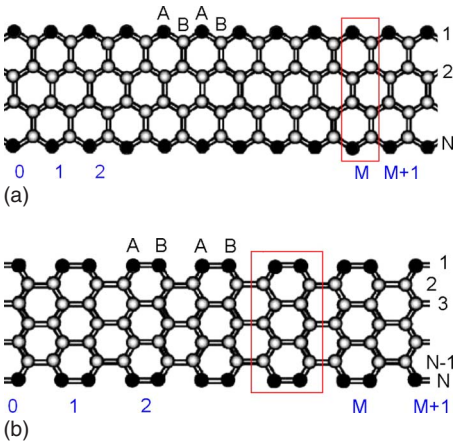

FIG. 1. (Color online) Geometry of graphene ribbons. (a) A zigzag ribbon ($N=4$); (b) an armchair ribbon ($N=7$). A black circle denotes an edge carbon and a gray circle denotes a bulk carbon. A unit cell contains $2N$ atoms. From the top down, atoms in a unit cell are labeled as 1A, 1B, 2A, 2B, …, NA, NB. Atoms close to 1B are 1A and 2A, and so on.

In our calculation, external electrodes and the central part (sample) are assumed to be made of GNRs. Moreover, the edge defects are modeled by appropriate on-site (diagonal) energy in the Hamiltonian of the sample. We utilize a quick iterative scheme[32,33] to calculate the surface Green's functions of electrodes and an efficient recursive algorithm[32,34] to calculate the total Green's function of the whole system. Finally, the conductance is calculated by the Landauer formula.[35,36] The calculation time of this method is only linearly dependent on the length of the sample and a GNR with disorder distributed over a length of 1 μm is tractable.

We first study the conductance of zigzag and armchair GNRs with the simplest possible edge defects, a single vacancy or a weak scatter. Then we use a simple one-dimensional (1D) model to explain the zero-conductance dips caused by edge defects. Finally, we study some more realistic structures, GNRs with weak scatters randomly distributed on their edges. We find that a weak disorder can change zigzag ribbons from metallic to semiconducting, but only changes the conductance of armchair ribbons slightly. The paper is organized as follows: in Sec. II, we introduce the model and method employed in this paper. Results and discussion are presented in Sec. III. We conclude our findings in Sec. IV.

II. MODEL AND METHOD

The geometry of GNRs is shown in Fig. 1. A graphene ribbon contains two unequal sublattices, denoted by A and B

in this paper. We use N, the number of A(B)-site atoms in a unit cell, to denote GNRs with different widths.[18] Then the widths of ribbons with zigzag edges and armchair edges are $W_z=\sqrt{3}Na_0/2$ and $W_a=Na_0/2$, respectively, where $a_0=2.49$ Å is the graphene lattice constant. The length is $L_z=Ma_0$ for a zigzag ribbon, and $L_a=\sqrt{3}Ma_0$ for an armchair ribbon, where M is the number of unit cells of the ribbon. From the top down, atoms in a unit cell will be labeled as 1A, 1B, …, NA, NB. As shown in Fig. 1, an edge atom is a carbon atom at the edge of GNRs that is connected by only two other carbon atoms. In this paper, we consider defects that locate at the sites of these edge atoms only.

The system under consideration is composed of two electrodes and a central part (sample). The sample (unit cells 1, …, M) is a finite GNR, which may contain edge defects, while the left and right electrodes are assumed to be semi-infinite perfect GNRs. We describe the GNR by a tight-binding model with one π-electron per atom. The tight-binding Hamiltonian of the system is

$$H=\sum_i \varepsilon_i a_i^\dagger a_i - V_{pp\pi}\sum_{\langle i,j\rangle} a_i^\dagger a_j + \text{c.c.}, \tag{1}$$

where ε_i is the on-site energy and $V_{pp\pi}$ is the hopping parameter. The sum in $\langle i,j\rangle$ is restricted to the nearest-neighbor atoms. In the absence of defects, ε_i is taken to be zero and $V_{pp\pi}=2.66$ eV.[25] In the presence of defects, both the on-site energy and the hopping parameter can change. Here, we only consider the variation in the on-site energy. A vacancy is simulated by setting its on-site energy to infinity.[25,37] A weak scatter caused by impurity or distortion will be simulated by setting ε_i to a small value V_i. In the case of a weak disorder, V_i is randomly selected from the interval $\pm|V_d|$ for every edge atom.

In what follows we show how to calculate the conductance of the GNRs:

First, the surface retarded Green's functions of the left and right leads ($g_{0,0}^L, g_{M+1,M+1}^R$) are calculated by[32,33,38]

$$g_{0,0}^L=[E^+I-H_{0,0}-H_{-1,0}^\dagger\tilde{\Lambda}]^{-1}, \tag{2}$$

$$g_{M+1,M+1}^R=[E^+I-H_{0,0}-H_{-1,0}\Lambda]^{-1}, \tag{3}$$

where $E^+=E+i\eta$ ($\eta\to 0^+$) (Ref. 39) and I is a unit matrix. $H_{0,0}$ is the Hamiltonian of a unit cell in the lead, and $H_{-1,0}$ is the coupling matrix between two neighbor unit cells in the lead. Here Λ and $\tilde{\Lambda}$ are the appropriate transfer matrices, which can be calculated from the Hamiltonian matrix elements via an iterative procedure[33,40]

$$\Lambda=t_0+\tilde{t}_0t_1+\tilde{t}_0\tilde{t}_1t_2+\cdots+\tilde{t}_0\tilde{t}_1\tilde{t}_2\cdots t_n, \tag{4}$$

$$\tilde{\Lambda}=t_0+t_0\tilde{t}_1+t_0t_1\tilde{t}_2+\cdots+t_0t_1t_2\cdots\tilde{t}_n, \tag{5}$$

where t_i and $\tilde{t}_i$ are defined via the recursion formulas

$$t_i=(I-t_{i-1}\tilde{t}_{i-1}-\tilde{t}_{i-1}t_{i-1})^{-1}t_{i-1}^2, \tag{6}$$

$$\tilde{t}_i=(I-t_{i-1}\tilde{t}_{i-1}-\tilde{t}_{i-1}t_{i-1})^{-1}\tilde{t}_{i-1}^2, \tag{7}$$

and

$$t_0=(E^+I-H_{0,0})^{-1}H_{-1,0}^\dagger, \tag{8}$$

$$\tilde{t}_0=(E^+I-H_{0,0})^{-1}H_{-1,0}. \tag{9}$$

The process is repeated until $t_n,\tilde{t}_n\leqslant\delta$ with δ arbitrarily small.

Second, including the sample as a part of the right lead layer by layer (from $l=M$ to $l=2$), the new surface Green's functions are found by[32,34]

$$g_{l,l}^R=[E^+I-H_{l,l}-H_{l,l+1}g_{l+1,l+1}^RH_{l,l+1}^\dagger]^{-1}. \tag{10}$$

Third, the total Green's function $G_{1,1}$ can then be calculated by

$$G_{11}=[E^+I-H_{1,1}-\Sigma^L-\Sigma^R]^{-1}, \tag{11}$$

where

$$\Sigma^L=H_{0,1}^\dagger g_{0,0}^L H_{0,1}, \tag{12}$$

$$\Sigma^R=H_{1,2}g_{2,2}^RH_{1,2}^\dagger \tag{13}$$

are the self-energy functions due to the interaction with the left and right sides of the structure. From Green's function, the local density of states (LDOS) at site j can be found:

$$n_j=-\frac{1}{\pi}\,\text{Im}[G_{(j,j)}], \tag{14}$$

where $G_{(j,j)}$ is the matrix element of Green's function at site j.

Finally, the conductance $G_{(E)}$ of the graphene ribbon can be calculated using the Landauer formula[35,36]

$$G_{(E)}=\frac{2e^2}{h}T_{(E)}. \tag{15}$$

Here $T_{(E)}$ is the transmission coefficient, which can be expressed as[41,42]

$$T_{(E)}=\text{Tr}[\Gamma^LG_{11}\Gamma^RG_{11}^\dagger], \tag{16}$$

where

$$\Gamma^{L,R}=i[\Sigma^{L,R}-(\Sigma^{L,R})^\dagger]. \tag{17}$$

In this calculation, no matrix larger than $2N\times 2N$ is involved. Moreover, its cost is only linearly dependent on the length of the GNRs. This method has been used to study the effects of dangling ends on the conductance of side-contacted CNTs.[32] We have also calculated the band structures of perfect GNRs by diagonalizing the Hamiltonian. The conductances of perfect GNRs agree with the band structures.

III. RESULTS AND DISCUSSION

The electronic properties of GNRs are strongly dependent on their geometry. There are two basic shapes of regular graphene edges, namely, zigzag and armchair edges, depending on the cutting direction of the graphene sheet (see Fig. 1). All ribbons with zigzag edges (zigzag ribbons) are metal-

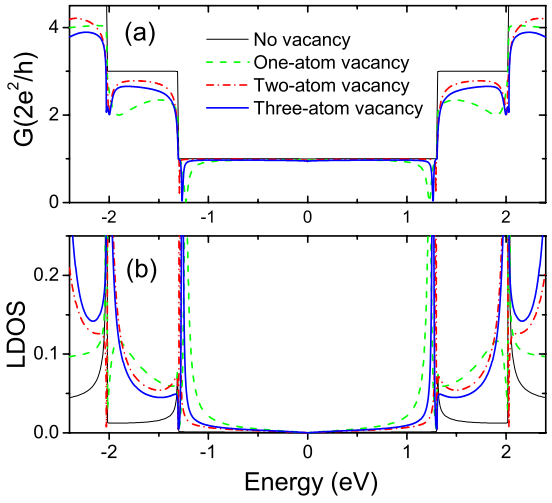

FIG. 2. (Color online) (a) Conductance of a zigzag ribbon ($N=8$, $W=17.3$ Å) without vacancy (thin solid line), and when one atom (1A), a pair of atoms (1A and 1B), and nearest three atoms (1A, 1B, and 1A) at its edge are removed. (b) LDOS of a 1B atom when there is no vacancy (thin solid line) and when there is a vacancy near it, corresponding to (a).

lic; however, two-thirds of ribbons with armchair edges (armchair ribbons) are semiconducting.[18,19] The bands of zigzag GNRs are partially flat around Fermi energy ($E_F=0$ eV),[18] which means the group velocity of mobile electrons is close to zero. On the other hand, the bands of metallic armchair GNRs are linear around Fermi energy.[18,27] So the group velocity of their mobile electrons around Fermi energy should be a constant value, which is measured to be about 10^6 m/s.[2] Since zigzag GNRs and armchair GNRs have so different electronic properties, the effects of edge defects on their conductance should also be very different.

A. Single defects

In this section, we will study the conductance and LDOS of GNRs with some single edge defects. A study of the effects of a single defect is not only realistic (e.g., a single two-atom vacancy at an armchair edge has been observed),[27] but also can serve as a guide for us to understand the effects of more complex edge defects.

1. Single vacancies

One of the simplest defects in a zigzag GNR is a single vacancy caused by the loss of one or several nearest edge atoms. In Fig. 2(a), we plot the conductance of a zigzag GNR ($N=8$) with a single one-atom vacancy (dashed line), a two-atom vacancy, and a three-atom vacancy as a function of the energy. The thin solid line is for the perfect GNR. These defects almost do not affect the conductance around the Fermi energy. There are two conductance dips close to the first band edges and simultaneously two peaks appear in the LDOS of the 1B atom near the vacancy [dashed line in Fig. 2(b)]. These two peaks have energies different from Van Hove singularities of a perfect GNR, which are extreme

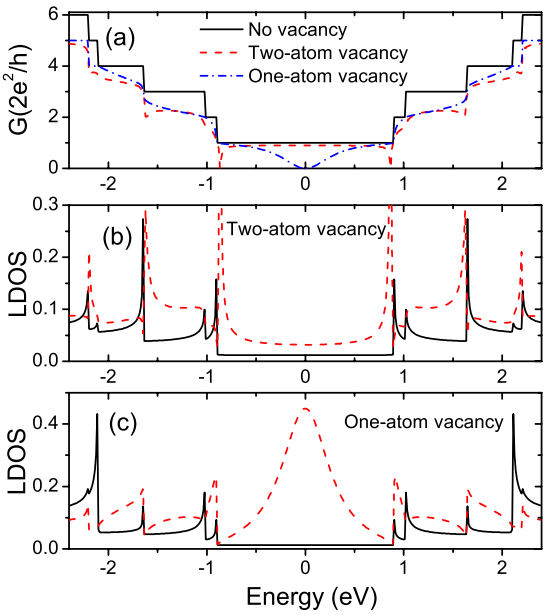

FIG. 3. (Color online) (a) Conductance of an armchair ribbon ($N=14$, $W=17.4$ Å) without vacancy (solid line), with a two-atom vacancy (dashed line), and with a one-atom vacancy (dash dot line) at its edge. (b) LDOS of a 2B atom when there is no vacancy (solid line) and when its nearest (1A and 1B) pair atoms are removed (dashed line). (c) LDOS of a 1B atom when there is no vacancy (solid line) and when its nearest 1A atom is removed (dashed line).

points of the 1D energy bands; so they are quasilocalized states caused by the vacancy. Moreover, the conductance dips are due to the antiresonance of these quasilocalized states. The relation between the conductance and quasilocalized states will be discussed further in Sec. III A 3.

The conductance and LDOS of armchair GNRs are displayed in Fig. 3. In an armchair GNR, edge atoms appear in pairs. A "single vacancy" can be formed by the loss of one edge atom (one-atom vacancy) or a pair of nearest edge atoms (two-atom vacancy). These two types of vacancies have very different properties especially around the Fermi energy. For the two-atom vacancy, the conductance is similar to that of the single vacancy situation of the zigzag ribbon, as well as the LDOS. However, when there is a one-atom vacancy, a large LDOS will be formed and consequently a large conductance dip will appear at the Fermi energy. In fact, it is expected that the effect of a one-atom vacancy is much larger than a two-atom vacancy because a one-atom vacancy breaks the symmetry between the two sublattices, while a two-atom vacancy keeps such symmetry. This is the same as in CNTs.

The conductance around the Fermi energy is a very important parameter for the application of GNRs. It is affected by edge defects shown above. Also it depends on the width of the ribbon. For example, a one-atom vacancy at the edge of an armchair GNR will always cause a zero-conductance dip at the Fermi energy. However, the breadth of the dip will change when the width of GNR changes. In order to describe the effect of a defect on the conductance quantitatively, we introduce the decreasing rate of the average conductance, which is

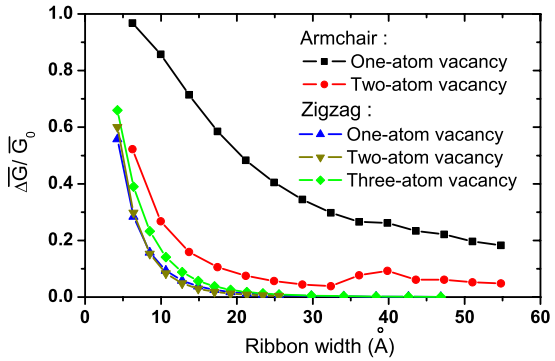

FIG. 4. (Color online) The decreasing rate of the average conductance (between ±0.5 eV) due to a single vacancy at the edge. As the width of a zigzag ribbon increases, its conductance becomes immune from a vacancy at its edge.

$$\overline{\Delta G}/\overline{G_0} = \frac{\int_{-\Delta E}^{\Delta E} [G_0(E) - G(E)]\mathrm{d}E}{\int_{-\Delta E}^{\Delta E} G_0(E)\mathrm{d}E}, \tag{18}$$

where $G_0(E)$ is the conductance of a GNR without defects and $G(E)$ is the conductance of the GNR with a defect. The decreasing rate of the average conductance (between ±0.5 eV) as a function of the ribbon width is plotted in Fig. 4. From the figure, we know that edge vacancies affect armchair GNRs much more strongly than zigzag GNRs. Moreover, the effect of edge vacancies decreases when the width of GNRs increases. This is because there are more atoms in the cross section of a wider GNR, so electrons are easier to go around the defect. Thus we can use wide GNRs as connections in a nanodevice to avoid the change of conductance due to edge vacancies. There is a small bump in $\overline{\Delta G}/\overline{G_0}$ of armchair GNRs with a two-atom vacancy at 40 Å. It is because the conductance dips at band edges (Fig. 3) enter into the energy range of ±0.5 eV as the width of GNRs increases. This does not change the overall decreasing tendency of $\overline{\Delta G}/\overline{G_0}$ when the width of GNRs increases.

2. Single weak scatters

Another kind of single defect is a weak scatter, which can be caused by a local lattice distortion, an absorption of an impurity atom at the edge, or a substitution of a carbon atom by an impurity atom. A weak scatter will modify the local distribution of charges, which changes the on-site energy; so we can simulate a single weak scatter by changing the on-site energy of an edge atom to a small defect potential V.

The conductances and LDOS of zigzag GNRs under the influences of single weak edge scatters with different strengths are presented in Figs. 5(a) and 5(b). It can be seen that even a very weak edge scatter (V=0.5 eV) can produce a quasilocalized state around Fermi energy (0.1 eV) and cause a zero-conductance dip. Moreover, the energy level and breadth of the dip increase when the defect potential increases. This is because the kinetic energy of mobile electrons in a zigzag GNR is nearly zero around Fermi energy.

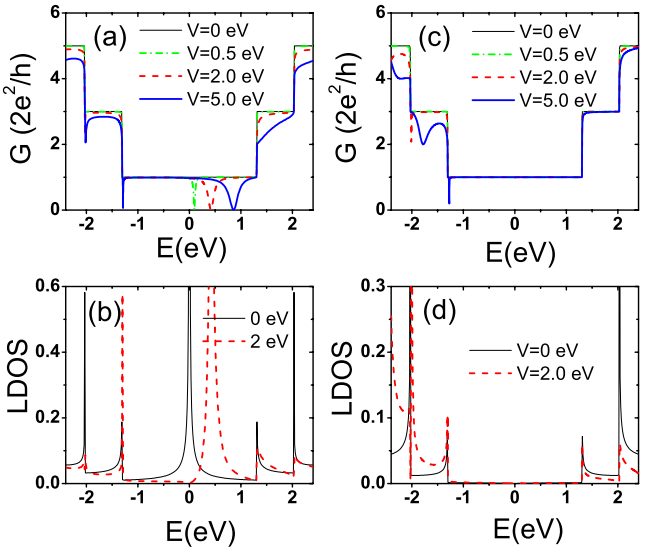

FIG. 5. (Color online) (a) Conductance of a zigzag ribbon (N=8) for various strengths of defect potential when the ribbon has a weak scatter at its edge. (b) The LDOS of an edge atom for V=0 eV (no defect) and V=2.0 eV at that site. (c) Conductance of a zigzag ribbon (N=8) when there is a weak scatter at its 1B site (not an edge atom). (d) The LDOS of a 1B atom for V=0 eV and V=2.0 eV at that site.

Moreover, these mobile electrons are localized to ribbon edges (edge states),[18] so they can be easily reflected by a weak scatter at the edge. The edge state at a zigzag edge has a nonbonding character.[18] The bulk site 1B is a node site of the wave function, so a weak scatter at site 1B has few effects on the conductance [see Figs. 5(c) and 5(d)]. Edge states with energies about −0.1 to 0.2 eV have been observed.[27,28] These correspond to weak scatters with defect potential from −0.52 to 0.98 eV for a N=8 zigzag ribbon, or from −0.46 to 0.93 eV for a N=22 zigzag ribbon. The energy level of a quasilocalized state does not depend very much on the width of the GNR, but the breadth of the state is much smaller for a wider GNR.

There is also no conductance dip near Fermi energy for armchair GNRs with a weak scatter. Moreover, the conductance dip at the band edge only becomes visible when the defect potential is larger than 2.0 eV (see Fig. 6). This is because the group velocity of mobile electrons in armchair GNRs around Fermi energy is in the order of 10^6 m/s, which gives a large kinetic energy; so these mobile electrons will not be sensitive to a weak edge scatter as those in zigzag GNRs.

3. Simple one-dimensional model

There are some common characters in the conductance curves and LDOS curves shown above (Figs. 2, 3, 5, and 6). First, there are sharp peaks in LDOS curves of perfect GNRs, which are Van Hove singularities (VHSs) corresponding to extreme points in the energy bands. VHSs are characteristic of the dimension of a system. In three-dimensional systems, VHSs are kinks due to the change in the degeneracy of the available phase space, while in 2D systems, the VHSs appear

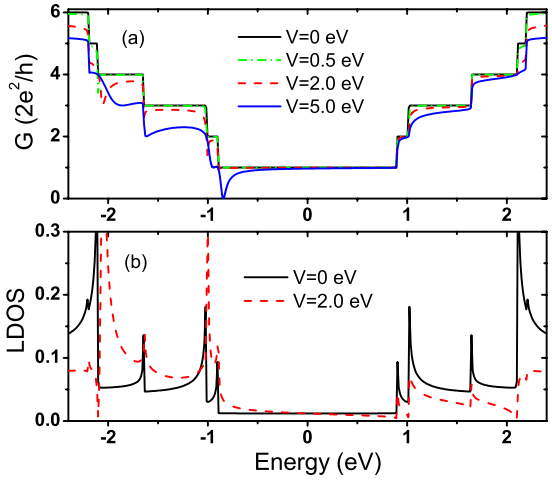

FIG. 6. (Color online) (a) Conductance of an armchair ribbon ($N=14$) for various strengths of defect potential when the ribbon has a weak scatter at its edge. (b) The LDOS of an edge atom for $V=0$ eV (no defect) and $V=2.0$ eV at that site.

as stepwise discontinuities with increasing energy.[43] Unique to 1D systems, the VHSs display as peaks; so GNRs are expected to exhibit sharp peaks in the LDOS due to the 1D nature of their band structures. Second, besides these VHSs, there are new peaks in the LDOS of GNRs with an edge defect. Moreover, zero-conductance dips occur at the same energy of these new peaks simultaneously. These new peaks in LDOS only occur near the defect, but have effects on the conductance of GNRs; so they correspond to quasilocalized states. Moreover, the zero-conductance dips are due to the antiresonance of these quasilocalized states. The relation between quasilocalized states and zero-conductance dips can be understood by a simple 1D model.

A GNR with an edge defect which induces a quasilocalized state (QLS) can be modeled as a 1D quantum wire (QW) with a side quantum dot (see Fig. 7). The quantum wire has one conducting band with dispersion relation $E=2\nu\cos(kd)$, where E is the energy of electrons, ν the hopping coefficient in the QW, and d the lattice spacing. The energy level of the quasilocalized state (side quantum dot) is ε_L. Moreover, the coupling between the quasilocalized state and the QW is t_{LC}. If $t_{LC}=0$, the state is completely localized and has no effect on the conductance of the QW. When $t_{LC}\neq 0$, the electrons not only can transport in the QW, but also can transport through "QW→QLS→QW," "QW→QLS→QW→QLS→QW," and so on. These different channels will interfere with each other and can cause resonance or antiresonance. It is easy to show that they will always cause antiresonance.[44]

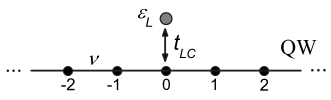

FIG. 7. A one-dimensional model of a system including conducting bands and a quasilocalized state (QLS). The bulk of the system is represented by a quantum wire (QW), which has one conducting band.

To calculate the conductance of this simple system, we assume that the electrons are described by a plane wave incident from the far left with unity amplitude and a reflection amplitude r and at the far right by a transmission amplitude t; so the probability amplitude to find the electron in the site j of the QW in the state k can be written as

$$a_j^k = e^{ikdj} + re^{-ikdj}, \quad j<0, \tag{19}$$

$$a_j^k = te^{ikdj}, \quad j>0. \tag{20}$$

Then the transmission amplitude t and thus the conductance of the system can be easily calculated by its tight-binding Hamiltonian.[44] The conductance is

$$G_{(E)} = \frac{2e^2}{h}\frac{1}{1+\dfrac{t_{LC}^4}{4\nu^2\sin^2(kd)(E-\varepsilon_L)^2}}. \tag{21}$$

From Eq. (21), we can see that when $E=\varepsilon_L$, the conductance G will be zero and a dip will appear in the conductance curve. In other words, the incident electrons will be totally reflected when their energy is equal to the energy level of the quasilocalized state; so the quasilocalized state causes an antiresonance. This analytical result agrees with our numerical results of GNRs. This relation between the conductance dips and localized states is very useful in experiments. It is not easy to measure the conductance of GNRs directly because of their small size. However, the quasilocalized states can be found in the scanning tunneling spectroscopy (STS) images or low bias scanning tunneling microscopy (STM) images.[27] Then with a STS image or a low bias STM image, the conductance dips can be predicted.

B. Weak disorders

Experimental observed graphene edges[10,27,28] have a lot of defects due to imperfect cutting. Most of these defects are likely to be avoided in the future with improvements in the processing of GNRs. However, as all materials have defects, real GNRs will always have some randomly distributed scatters at their edges due to lattice distortion or impurity. In this section, we will consider the properties of GNRs under the influence of weak uniform disorders at their edges. An edge disorder distributed over a length L will be simulated by setting the on-site energies of all edge atoms within a length L to energies randomly selected from the interval $\pm|V_d|$, where $|V_d|$ is the disorder strength.

The conductances of zigzag GNRs with different disorder strengths and distribution lengths are displayed in Fig. 8. The most important feature of the conductance curves is that there are gaps around the Fermi energy. For a $N=8$ zigzag GNR with a very weak disorder ($V_d=0.25$ eV) distributed over a length 1000 Å, the conductance has a 0.25 eV gap, within which its maximum is less than 10^{-3} of $(2e^2/h)$. If the disorder strength is 1.0 eV, the conductance gap is 1.04 eV. This is enormous because a semiconducting perfect GNR with a similar width only has a gap less than 0.7 eV.[19,20]

The conductance gaps around the Fermi energy come from the Anderson localization of electrons.[45–47] In a perfect

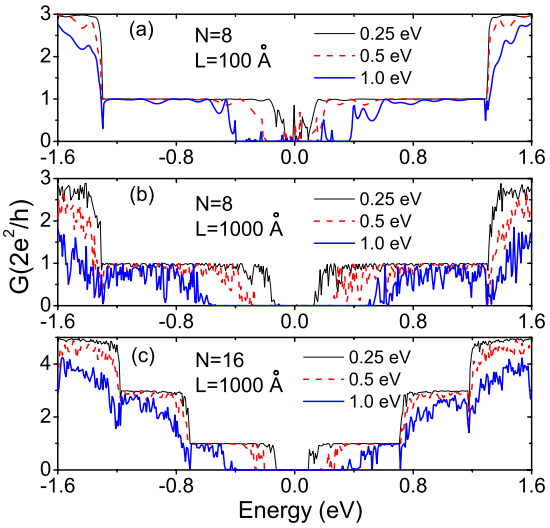

FIG. 8. (Color online) Conductance versus energy for zigzag ribbons ($N=8,16$) with disorder distributed at both edges over lengths of 100 and 1000 Å. With a weak disorder, zigzag GNRs change from metallic to semiconducting.

GNR or a GNR with periodic defects, the constructive interference of tunneling allows that electrons within certain energy bands can propagate through an infinite GNR (Bloch tunneling). However, the disorder can disturb the constructive interference sufficiently to localize electrons. In an infinite 1D system, even weak disorder localizes all states, yielding zero conductance. If the disorder is only distributed within a finite length L, the conductance is expected to decrease exponentially with length, $G=G_0\exp(-L/L_0)$, when L is much larger than localization length L_0.[48,49] We observe this is true in our simulations [see Fig. 9(a)]. Each point in Fig. 9 is an average over several thousand disorder configurations. The localization length of electrons with energy close to zero is very small in the zigzag ribbons. From the top down, the fitted localization lengths are $L_0=59$ Å, $L_0=51$ Å, $L_0=53$ Å, and $L_0=45$ Å for curves in Fig. 9(a), respectively; so the wider the ribbon, the longer the localization length. Moreover, the stronger the disorder strength, the shorter the localization length.

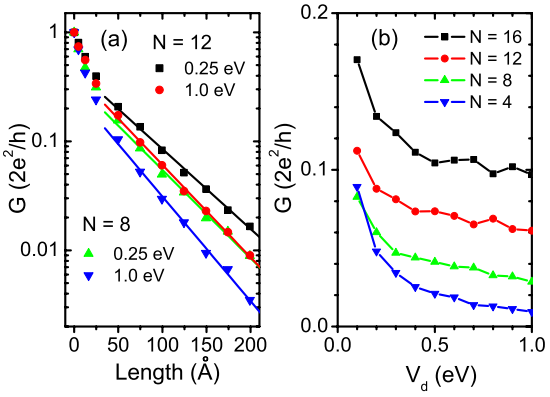

FIG. 9. (Color online) (a) Conductance versus ribbon length for two zigzag ribbons ($N=8,12$) with different disorder strengths ($V_d=0.25$, 1.0 eV). The straight lines are exponential fits to the simulated data with the ribbon length larger than 50 Å. (b) Conductance versus disorder strength for zigzag ribbons with disorder distributed at both edges over a length of 100 Å.

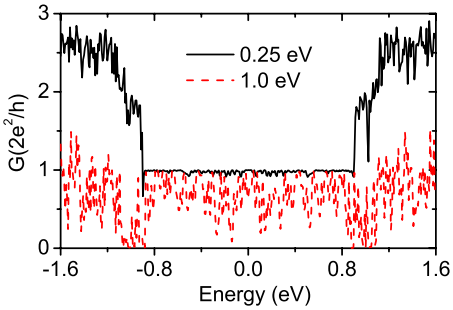

FIG. 10. (Color online) Conductance versus energy for an armchair ribbon ($N=14$) with disorder distributed at its both edges over a length of 1000 Å.

The conductance of the armchair GNRs with weak disorders is plotted in Fig. 10. Unlike the conductance of zigzag ribbons, there is no gap around the Fermi energy. We also calculate the conductance versus disorder length, which is shown in Fig. 11(a). The conductance also decreases exponentially but much slower. The $N=14$ armchair GNRs ($W=17.4$ Å) have nearly the same width of $N=8$ zigzag GNRs ($W=17.3$ Å). However, their localization lengths are very different. When the disorder strength is $V_d=0.25$ eV, the localization length of $N=14$ armchair GNRs is larger than 2 μm, while $L_0=59$ Å for $N=8$ zigzag GNRs. So the localization is much weaker in armchair GNRs than in zigzag GNRs. As discussed in Sec. III A, this is because the kinetic energy of mobile electrons around Fermi energy in armchair GNRs is larger than in zigzag GNRs, and also because these mobile electrons in zigzag GNRs are localized to edges, while they distribute in the whole cross section of armchair GNRs; so when compared to zigzag GNRs, armchair GNRs are more like 2D systems where electrons are easier to travel around defects. There is no such difference between zigzag

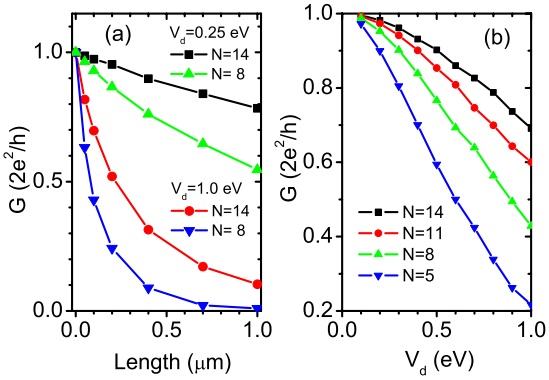

FIG. 11. (Color online) (a) Conductance versus ribbon length for two armchair ribbons ($N=8,14$) with different disorder strengths. (b) Conductance versus disorder strength for armchair ribbons with disorder distributed at both edges over a length of 1000 Å.

and armchair CNTs. The conductances of both zigzag CNTs and armchair CNTs are not significantly affected by disorder.[26] Figure 11(b) shows the conductance versus disorder strength for armchair GNRs. The conductance of narrow GNRs decreases very fast when the disorder strength increases.

Recent studies of perfect GNRs have found that, with edge corrections which keep the translational symmetry of GNRs, all zigzag GNRs will be still metallic.[19] Here we show that with a weak disorder at edges, zigzag GNRs will change from metallic to semiconducting due to Anderson localization; so narrow zigzag GNRs with a weak disorder can be used as functional elements in a nanodevice. This result is important because nearly all realistic GNRs contain some edge disorder.

IV. CONCLUSION

Using a tight-binding model, we have investigated the conductance of the zigzag and armchair graphene nanoribbons with single defects or weak disorder at their edges. We first study the simplest possible edge defects, a single vacancy or a weak scatter. We find that even these simplest defects have highly nontrivial effects. A single edge defect will induce quasilocalized states and consequently cause zero-conductance dips. Moreover, the center energies and breadths of such dips are strongly dependent on the geometry of GNRs. A one-atom edge vacancy will completely reflect electrons at Fermi energy in an armchair GNR, while only slightly affecting the transport of electrons in a zigzag GNR. The effect of a two-atom vacancy in an armchair GNR is similar to the effect of a one-atom vacancy in a zigzag GNR. A weak scatter can cause a quasilocalized state and consequently a zero-conductance dip near Fermi energy in a zigzag GNR. However, its effect on the conductance of armchair ribbons near Fermi energy is negligible. The influence of edge defects on the conductance will decrease when the widths of GNRs increase. Then we use a simple one-dimensional model to discuss the relation between quasilocalized states and zero-conductance dips of GNRs. We find that a quasilocalized state caused by a defect will cause antiresonance and corresponds to a zero-conductance dip.

Finally, we study some more realistic structures, GNRs with weak scatters randomly distributed on their edges. We find that with a weak disorder distributed in a finite length, zigzag GNRs will change from metallic to semiconducting due to Anderson localization. However, a weak disorder only slightly affects the conductance of armchair GNRs. The effect of edge disorder decreases as the width of GNRs increases; so narrow zigzag GNRs with a weak disorder can be used as field-effect transistors in a nanodevice. Moreover, GNRs used as connections should be wider than GNRs used as functional elements. These results are useful for better understanding the property of realistic graphene nanoribbons, and will be helpful for designing nanodevices based on graphene in the future.

ACKNOWLEDGMENT

The authors would like to thank N. M. R. Peres for helpful discussions.

[1] K. S. Novoselov, A. K. Geim, S. V. Morozov, D. Jiang, Y. Zhang, S. V. Dubonos, I. V. Grigorieva, and A. A. Firsov, Science **306**, 666 (2004).
[2] K. S. Novoselov, A. K. Geim, S. V. Morozov, D. Jiang, M. I. Katsnelson, I. V. Grigorieva, S. V. Dubonos, and A. A. Firsov, Nature (London) **438**, 197 (2005).
[3] P. R. Wallace, Phys. Rev. **71**, 622 (1947).
[4] Y. Zhang, Y.-W. Tan, H. L. Stormer, and P. Kim, Nature (London) **438**, 201 (2005).
[5] V. P. Gusynin and S. G. Sharapov, Phys. Rev. Lett. **95**, 146801 (2005).
[6] N. M. R. Peres, F. Guinea, and A. H. Castro Neto, Phys. Rev. B **73**, 125411 (2006).
[7] I. L. Aleiner and K. B. Efetov, Phys. Rev. Lett. **97**, 236801 (2006).
[8] A. H. Castro Neto, F. Guinea, and N. M. R. Peres, Phys. Rev. B **73**, 205408 (2006).
[9] A. H. Castro Neto, F. Guinea, N. M. R. Peres, K. S. Novoselov, and A. K. Geim, arXiv:0709.1163 (unpublished).
[10] S. Banerjee, M. Sardar, N. Gayathri, A. K. Tyagi, and B. Raj, Phys. Rev. B **72**, 075418 (2005).
[11] K. Wakabayashi, Phys. Rev. B **64**, 125428 (2001).
[12] Z. Chen, Y.-M. Lin, M. J. Rooks, and P. Avouris, Physica E (Amsterdam) **40**, 228 (2007).
[13] M. Y. Han, B. Özyilmaz, Y. Zhang, and P. Kim, Phys. Rev. Lett. **98**, 206805 (2007).
[14] B. Özyilmaz, P. Jarillo-Herrero, D. Efetov, and P. Kim, Appl. Phys. Lett. **91**, 192107 (2007).
[15] C. Stampfer, J. Güttinger, F. Molitor, D. Graf, T. Ihn, and K. Ensslin, Appl. Phys. Lett. **92**, 012102 (2008).
[16] M. Wilson, Phys. Today **59**(1), 21 (2006).
[17] J. Fernández-Rossier, J. J. Palacios, and L. Brey, Phys. Rev. B **75**, 205441 (2007).
[18] K. Nakada, M. Fujita, G. Dresselhaus, and M. S. Dresselhaus, Phys. Rev. B **54**, 17954 (1996).
[19] M. Ezawa, Phys. Rev. B **73**, 045432 (2006).
[20] L. Brey and H. A. Fertig, Phys. Rev. B **73**, 235411 (2006).
[21] K. Wakabayashi and M. Sigrist, Phys. Rev. Lett. **84**, 3390 (2000).
[22] B. Obradovic, R. Kotlyar, F. Heinz, P. Matagne, T. Rakshit, M. D. Giles, M. A. Stettler, and D. E. Nikonov, Appl. Phys. Lett. **88**, 142102 (2006).
[23] Z. Yao, H. W. C. Postma, L. Balents, and C. Dekker, Nature (London) **402**, 273 (1999).
[24] Z. Chen, J. Appenzeller, Y.-M. Lin, J. Sippel-Oakley, A. G. Rinzler, J. Tang, S. J. Wind, P. M. Solomon, and P. Avouris, Science **311**, 1735 (2006).
[25] L. Chico, L. X. Benedict, S. G. Louie, and M. L. Cohen, Phys. Rev. B **54**, 2600 (1996).
[26] M. P. Anantram and T. R. Govindan, Phys. Rev. B **58**, 4882 (1998).

[27] Y. Kobayashi, K.-I. Fukui, T. Enoki, and K. Kusakabe, Phys. Rev. B **73**, 125415 (2006).
[28] Y. Niimi, T. Matsui, H. Kambara, K. Tagami, M. Tsukada, and H. Fukuyama, Phys. Rev. B **73**, 085421 (2006).
[29] M. Fujita, M. Igami, and K. Nakada, J. Phys. Soc. Jpn. **66**, 1864 (1997).
[30] Y. Miyamoto, K. Nakada, and M. Fujita, Phys. Rev. B **59**, 9858 (1999).
[31] F. Muñoz-Rojas, D. Jacob, J. Fernández-Rossier, and J. J. Palacios, Phys. Rev. B **74**, 195417 (2006).
[32] T. Li, Q. W. Shi, X. Wang, Q. Chen, J. Hou, and J. Chen, Phys. Rev. B **72**, 035422 (2005).
[33] M. P. L. Sancho, J. M. L. Sancho, and J. Rubio, J. Phys. F: Met. Phys. **14**, 1205 (1984).
[34] S. Krompiewski, J. Martinek, and J. Barnaś, Phys. Rev. B **66**, 073412 (2002).
[35] Y. Imry and R. Landauer, Rev. Mod. Phys. **71**, S306 (1999).
[36] S. Datta, *Electronic Transport in Mesoscopic Systems* (Cambridge University Press, Cambridge, 1995).
[37] K. Wakabayashi, J. Phys. Soc. Jpn. **71**, 2500 (2002).
[38] J. Jiang, J. Dong, and D. Y. Xing, Phys. Rev. Lett. **91**, 056802 (2003).
[39] We use $\eta=10^{-4}$ eV for GNRs with a single defect and $\eta=10^{-6}$ eV for GNRs with a weak disorder.
[40] M. B. Nardelli, Phys. Rev. B **60**, 7828 (1999).
[41] D. S. Fisher and P. A. Lee, Phys. Rev. B **23**, 6851 (1981).
[42] Y. Meir and N. S. Wingreen, Phys. Rev. Lett. **68**, 2512 (1992).
[43] T. W. Odom, J. L. Huang, P. Kim, and C. M. Lieber, J. Phys. Chem. B **104**, 2794 (2000).
[44] P. A. Orellana, F. Dominguez-Adame, I. Gómez, and M. L. Ladrón de Guevara, Phys. Rev. B **67**, 085321 (2003).
[45] P. W. Anderson, Phys. Rev. **109**, 1492 (1958).
[46] B. Biel, F. J. García-Vidal, A. Rubio, and F. Flores, Phys. Rev. Lett. **95**, 266801 (2005).
[47] I. V. Gornyi, A. D. Mirlin, and D. G. Polyakov, Phys. Rev. Lett. **95**, 206603 (2005).
[48] P. A. Lee and T. V. Ramakrishnan, Rev. Mod. Phys. **57**, 287 (1985).
[49] C. W. J. Beenakker, Rev. Mod. Phys. **69**, 731 (1997).